

## Position-dependent expression of potassium currents by chick cochlear hair cells

B. W. Murrow

*Department of Physiology, University of Colorado Health Sciences Center,  
4200 East 9th Avenue, Denver, CO 80262, USA*

1. Potassium currents in chick cochlear hair cells were studied using whole-cell voltage clamp techniques. Cells were isolated from 200  $\mu\text{m}$ -long segments of the apical half of the cochlea. In each segment, expression of potassium currents by cells positioned across the width ('inner–outer' hair cell axis) of the cochlea was examined.
2. A rapidly inactivating potassium current ( $I_A$ ) was found in some hair cells. At a membrane potential of  $-24$  mV,  $I_A$  activated to peak values within  $7 \pm 1$  ms and inactivated within  $73 \pm 16$  ms. The activation 'threshold' was around  $-50$  mV and hyperpolarization more negative than  $-56 \pm 5$  mV was required before significant removal of inactivation occurred ( $V_{1/2}$  (half-inactivation potential) =  $-74 \pm 5$  mV). The resting potential of cells with  $I_A$  was  $-46$  mV  $\pm$  11 mV. This current was blocked by 4-aminopyridine with a  $K_d$  of 0.45 mM.
3. Cells that were isolated from the most apical tip of the cochlea expressed no  $I_A$ . In areas more basal than 200  $\mu\text{m}$  from the apex, the magnitude of  $I_A$  correlated with cell morphology. In each area, the tallest hair cells (cells with the smallest ratio of apical surface diameter to length) had none of this current. Of the cells with  $I_A$ , the shorter cells (larger ratio of apical surface diameter to length) had more of this current.
4. The magnitude of  $I_A$  in a cell was dependent upon cross-cochlear position, and the relationship between  $I_A$  and cell morphology was most probably a reflection of a differential distribution of cell shape across the cochlea. The tallest hair cells, occupying roughly the first 40% of the distance from the neural side of the basilar papilla, had no  $I_A$ . Of the remaining cells, those nearer to the abneural edge expressed more  $I_A$ , such that iso-magnitude lines ran approximately parallel to the long axis of the cochlea.
5. A delayed rectifier current ( $I_K$ ) and an inward rectifier current ( $I_{IR}$ ) were also differentially distributed among hair cells across the cochlea; however, their distribution differed from that of  $I_A$ .  $I_K$  and  $I_{IR}$  were preferentially expressed by the taller hair cells, which were positioned nearer to the neural side of the cochlea.  $\text{Ca}^{2+}$ -activated potassium current ( $I_{K(\text{Ca})}$ ) did not vary systematically between cells of different shape or cross-cochlear position, and  $I_{K(\text{Ca})}$  could often be found in cells with  $I_A$ .

The basilar papilla ('cochlea') of the chick contains roughly 10000 auditory receptor cells (hair cells) that form a slightly curved, spatula-shaped acoustic epithelium. At its widest point, forty-five hair cells span the width of the basilar papilla. The morphology, position, and innervation of the hair cells indicate that these cells can be divided into more than one type (Tanaka & Smith, 1978). The hair cells along one side of the basilar papilla (neural) are columnar, while the cells along the opposite side (abneural) are shorter with expanded apical surfaces. The morphology of the cells gradually changes across the cochlear width. Those cells with a length greater than their apical surface diameter have been termed tall hair cells (THCs), while those with a length less than their apical diameter have been called

short hair cells (SHCs) (Tanaka & Smith, 1978). The THCs receive the preponderance of afferent innervation, while the SHCs are more densely innervated by efferent fibres (Tanaka & Smith, 1978; Hirokawa, 1978). The characteristics of THCs and SHCs suggest that they are analogous to the inner and outer hair cells, respectively, of the mammalian cochlea. However, unlike the mammalian cochlea, the border between the classes of hair cells is not clearly delineated.

The types of ion channels expressed by the hair cell shape the receptor potential of the cell and thus control cell physiology. THCs express a variety of membrane currents that vary along the long axis (length) of the cochlea (Fuchs, Nagai & Evans, 1988; Fuchs & Evans,

1990). THCs from the middle third of the cochlear length were found to be electrically tuned by a voltage-dependent  $\text{Ca}^{2+}$  current ( $I_{\text{Ca}}$ ) and a  $\text{Ca}^{2+}$ -activated potassium ( $\text{K}^+$ ) current ( $I_{\text{K(Ca)}}$ ). Within this group, cells that were more basally located were tuned to higher frequencies and had  $I_{\text{K(Ca)}}$  with faster kinetics. THCs from the cochlear apex, while also exhibiting  $I_{\text{Ca}}$ , tended to express a slow  $\text{K}^+$  current of the delayed rectifier type ( $I_{\text{K}}$ ) in lieu of  $I_{\text{K(Ca)}}$ . Furthermore, these slow cells also often had large amounts of inward rectifier  $\text{K}^+$  current ( $I_{\text{IR}}$ ). Such cells had large negative resting potentials and response kinetics appropriate for sensing low frequencies of sound.

Much less is known about the physiology of SHCs. Hence, an electrophysiological study of the hair cells positioned across the cochlea was undertaken. Preliminary results (Murrow & Fuchs, 1990) found preferential expression of a rapidly inactivating potassium current ( $I_{\text{A}}$ ) and a cholinergic-activated current by SHCs. The present report elaborates on  $I_{\text{A}}$  in chick hair cells and compares its distribution of expression among cells to that of other current types, including  $I_{\text{K}}$ ,  $I_{\text{IR}}$  and  $I_{\text{K(Ca)}}$ .

## METHODS

### Electrophysiological experiments

All experiments were carried out on hair cells from cochleas of 2- to 4-week-old chicks (*Gallus domesticus*, Leghorn). Following decapitation, the head was bisected sagittally and a half-head was immediately placed into cold, oxygenated chick saline solution that contained (mM): 154 NaCl, 6 KCl, 5.6  $\text{CaCl}_2$ , 2.3  $\text{MgCl}_2$ , 5 HEPES and 8 glucose at pH 7.4. The cochlear dissection, via a medial approach, and isolation of the hair cells were performed according to Fuchs *et al.* (1988). The hair cells were isolated from well-defined areas in the cochlea. The basilar papilla was divided into 200  $\mu\text{m}$ -long sections that were numbered consecutively, starting at the most apical

segment (Fig. 1). Hair cells were isolated from only one section at a given time, providing positional information along the length of the cochlea for those cells. The recording dish was continuously perfused with fresh, oxygenated chick saline solution. All experiments were performed at room temperature, 22–25 °C. An inverted microscope (Optiphot-TMD, Nikon, Tokyo), modified for Hoffman differential-interference-contrast optics and equipped with a  $\times 40$  objective, was used to view the cells. The length and apical surface diameter of each cell were measured with an ocular micrometer before recording from the cell as discussed previously (Murrow & Fuchs, 1990).

**Electrical recordings.** Whole-cell clamp techniques (Marty & Neher, 1983) were used to examine the membrane currents and voltage of the isolated hair cells. Recording electrodes with tip resistances from 2 to 5  $\text{M}\Omega$  were made from borosilicate glass (Boralex disposable micropipettes, Rochester Scientific Co., Rochester, NY, USA) with a vertical puller (David Knopf Instruments). In order to reduce the electrode capacitance, the shank of the electrode was coated with cross-country ski wax (SWIX purple, Astra-Gruppen, A/S, Skärer, Norway). The electrode filling solution consisted of (mM): 112 KCl, 0.1  $\text{CaCl}_2$ , 2  $\text{MgCl}_2$ , 11 EGTA, 10 HEPES and 2 ATP (potassium salt) and was adjusted to a pH of 7.2 with KOH. An Axopatch 1A or Axoclamp 2B amplifier (Axon Instruments, Foster City, CA, USA) was used to record from the isolated hair cells. In voltage clamp, the Axopatch 1A permitted compensation (60–80%) for the series resistance, which ranged from 5 to 15  $\text{M}\Omega$  in these experiments. The Axoclamp 2B provided no means for such compensation. However, in experiments measuring the size of  $I_{\text{A}}$ , the current of interest was usually small (50–300 pA), and the effect of uncompensated series resistance was therefore small. Best estimates indicate an error of less than 4 mV in holding potentials and an error of less than 8% in determining  $I_{\text{A}}$  size. These small errors were not corrected for mathematically in the results. The time constant of the voltage clamp was better than 150  $\mu\text{s}$  in all recordings.

**Experimental solutions.** Identification of the types of current seen in voltage clamp recordings involved application of various experimental solutions (Table 1). All of the solutions

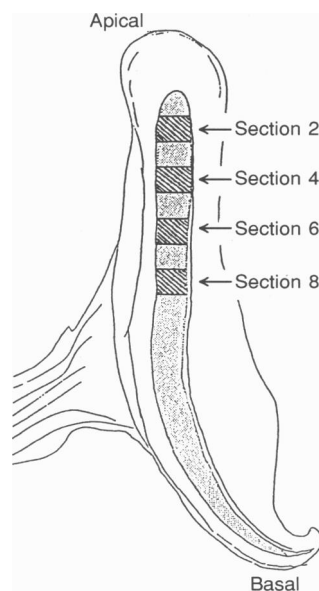


**Figure 1. Experimental division of basilar papilla into sections**

The shaded area in this drawing of a cochlea represents the basilar papilla, which includes the hair cells. Hair cells were isolated from the hatched sections, each spanning 200  $\mu\text{m}$  of the length of the cochlea.

Table 1. Experimental solutions (mM)

	NaCl	KCl	CaCl <sub>2</sub>	MgCl <sub>2</sub>
Chick (control) saline solution	154	6	5.6	2.3
10 mM TEA	144	6	5.6	2.3
Ca <sup>2+</sup> -free saline solution	154	6	—	7.9
10 mM 4-AP	144	6	5.6	2.3

were buffered with 5 mM Hepes and adjusted to a final pH of 7.4 by adding either NaOH or HCl. Different concentrations of 4-aminopyridine (4-AP) were made by substituting an equimolar amount of 4-AP for NaCl in chick (control) saline solution. Due to the instability of 4-AP when stored in solution (Thompson, 1977), fresh solutions were made up daily. An array of glass tubes with opening diameters of 50–80  $\mu\text{m}$  contained the solutions of interest and was positioned close to the cell (Yellen, 1982). Each tube was connected to a reservoir and turning the stopcock at the base of the reservoir rapidly surrounded the cell with the desired solution. One of the perfusion tubes contained chick saline solution as a control that was useful in rapidly reversing many of the test responses, which otherwise recovered much more slowly by bath perfusion alone.

**Isolation of currents.**  $I_A$  was isolated from other currents in the cell by either its sensitivity to 10 mM 4-AP (Fig. 2 in Murrow & Fuchs, 1990) or its voltage-dependent inactivation. The latter method involved subtracting the current in response to a depolarization from a holding potential of  $-44$  mV (Fig. 2) or  $-54$  mV (Fig. 3) from the response to the same potential from a hold of  $-84$  mV. Since  $I_A$  was inactivated at  $-44$  or  $-54$  mV and not at  $-84$  mV (see Results), the difference in current isolated  $I_A$  from the other non-inactivating currents.

The isolation of  $I_K$  and  $I_{K(\text{Ca})}$  from each other was based upon their kinetics of activation.  $I_{K(\text{Ca})}$  in chick hair cells is fully activated within 3 ms at  $-4$  mV (Fuchs & Evans, 1990), while only a small amount of  $I_K$  (the single exponential time constant for current rise ( $\tau$ )  $\approx 30$  ms) is activated in this time period. The magnitude of  $I_{K(\text{Ca})}$  activated at  $-4$  mV when stepped from  $-54$  mV was estimated as the amount of current present at 3 ms after the start of the step; any additional current generated after 3 ms was considered to be an estimate of the amount of  $I_K$  activated. Cells that revealed  $I_A$  under this voltage protocol were excluded for the purposes of these measurements.

$I_{\text{IR}}$  was measured as the steady-state current that was activated when the cell was held at  $-54$  mV and stepped to  $-94$  mV. Leakage current was adjusted for in these measurements.

**Data analysis.** Recordings from hair cells were stored on magnetic tape using a tape-recorder with a low-pass corner (3 dB) of 6.5 kHz at 15 in  $\text{s}^{-1}$  (Model 420b; Vetter, Petersburg, PA, USA) and analysed using DAOS version 7.0 (Laboratory Software Associated, Fitzroy, Victoria 3065, Australia) on an IBM 286 clone (AST Research Inc., Irvine, CA, USA) with Labmaster DMA TM-100 hardware (Scientific Solutions, Solon, OH, USA). Whenever possible, five traces of each current response were averaged to provide a representative sweep for that response. Membrane potentials were corrected for the junction potential (4 mV) between the internal (electrode) and external solution. Student's  $t$  test was used to

determine statistically significant differences between groups of data. Unless otherwise stated, all means are given with  $\pm$  the standard deviation.

### Morphological studies

**Experimental preparation.** Cochleas from 2- to 4-week-old chicks were prepared for light microscopy. Dissection of the cochlea was identical to that for electrophysiology experiments except that immediately after a portion of the bone overlying the cochlea was removed, the chick saline solution was replaced with 2.5% glutaraldehyde in 0.1 M sodium cacodylate at pH 7.2 for 2 h. The fixative was then replaced with chick saline solution and the dissection was continued. The isolated cochlea was further fixed in the glutaraldehyde solution overnight at 4 °C. On the following day, the specimen was rinsed with 0.1 M sodium cacodylate buffer and exposed to 1% osmium tetroxide in 0.1 M sodium cacodylate for 1 h on ice, followed by another rinse with the buffer. To *en bloc* stain the preparation, 2% uranyl acetate in 10% ethanol was used for 45 min. This was followed by three rinses in each of a graded ethanol series (50, 70, 95 and 100%) and then three 15 min changes of 100% acetone. The cochleas were infiltrated first with a 1:1 mixture of Spurr's epoxy resin (Electron Microscopy Science, Fort Washington, PA, USA) and acetone for 1 h, then with a 2:1 mixture of Spurr's and acetone, and finally with two changes of 100% Spurr's for 1 h each. The specimen was embedded and polymerized in a 60 °C oven for 24 h. Serial sections of the cochlea (4 or 8  $\mu\text{m}$  thick) were made using a Sorval MT2B ultramicrotome (Porter Blum, Ivan Sorval Inc., Newton, CT, USA) with a Dupont diamond knife or an Ultracut Ultra-microtome (Reichert, Vienna, Austria) with glass knives. The orientation of the cochlea was adjusted as needed so that the sections were perpendicular to the length of the curved basilar papilla as well as perpendicular to the apical surface of the hair cells. Sections were stained with 1% Toluidine Blue in 2.5% sodium carbonate, which clearly delineated the hair cells from surrounding supporting cells.

Two cochleas were serially sectioned. In one cochlea, two groups of ten 8  $\mu\text{m}$ -thick cross-sections, spanning 304–376 and 984–1056  $\mu\text{m}$  from the tip of the basilar papilla, were studied. In the other cochlea, two groups of eleven 4  $\mu\text{m}$ -thick cross-sections, spanning 260–304 and 1020–1068  $\mu\text{m}$ , were used. The areas examined in both of these cochleas corresponded to section 2 and section 6 (Fig. 1).

**Digitization.** The morphological parameters of hair cells in the serial cross-sections were determined. The sections were viewed with either a Nikon Optiphot microscope (total magnification  $\times 450$ ) or an American Optics microscope (Buffalo, NY, USA; total magnification  $\times 400$ ). Cell measurements were made using a camera lucida attachment on the scope and a digitizing pad connected to a computer (9874A Digitizer pad with a 9816 personal computer, Hewlett

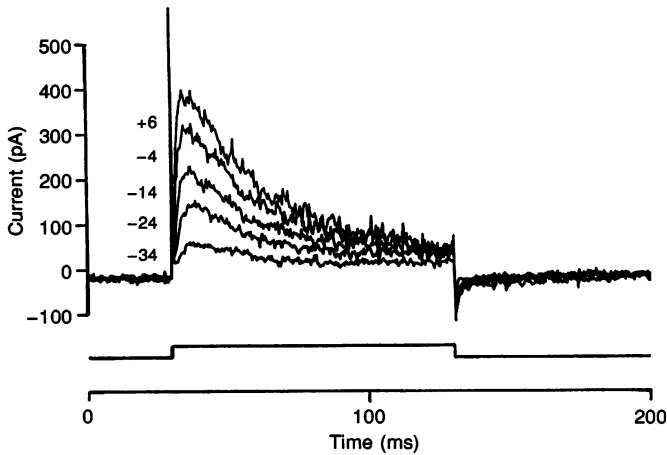


**Figure 2.**  $I_A$  at different membrane potentials.  $I_A$  was isolated from other membrane currents using its inactivating property as described in Methods. The square trace marks the timing of a 100 ms voltage step to the membrane potential (mV) that is indicated adjacent to each current trace. The small inward current preceding each voltage step is the difference in holding current at  $-84$  and  $-44$  mV.

Packard (Greeley, CO, USA), or a GP-7 Grafbardigitizer, Science Accessories Corp., Southport, CN, USA, connected to an IBM 286 clone). The length and apical surface diameter of each well-resolved cell were measured and the distance of the cell from the abneural edge of the basilar papilla was noted. Cells were only measured if they exhibited a hair bundle, a nucleus and a distinct basal end.

The hair cells from each of section 2 and 6 were divided into populations based upon distance across the cochlea. Data from cells located within the first 20% of the distance across the cochlea from the abneural side were pooled, similarly for the next 20%, and so on. The goal was to obtain a representative morphology of the cells in each of the final pooled populations. The representative apical diameter for each population of cells was taken as the maximal value measured from any cell of that population. This approach was necessary because the apical surface of the cells can be represented roughly by a circle and this circle was not always sectioned across its widest part; if the measurements were averaged, the apical surface diameter would be underestimated.

Even though extreme care was taken to section the hair cells parallel to their length, cells might still have been cut off this ideal axis and, as a result, could have been measured as shorter than their actual length. However, unlike the apical surface, a side view of the hair cells is not radially symmetrical, and therefore it is possible to also obtain a value for cell length that is larger than the actual length of the cell. To minimize this problem, a representative length for each population of cells was determined by averaging the values for all of the cells in that population.

## RESULTS

### Characteristics of a rapidly inactivating potassium current

In many cells, a rapidly inactivating outward current was observed during depolarizations from a holding potential of  $-84$  mV (Fig. 2). This current activated and inactivated during a maintained depolarization. The current was similar to A-type potassium currents ( $I_A$ ), first described in detail in molluscan neurons (Connor & Stevens, 1971). This current in chick hair cells was sensitive to 4-AP (Fig. 2 in Murrow & Fuchs, 1990), which blocks A-type potassium currents found in many preparations (reviewed by Rudy, 1988), including frog vestibular hair cells (Lewis & Hudspeth, 1983). Based upon these characteristics, the rapidly inactivating outward current in chick hair cells was also determined to be  $I_A$ .

Cells expressed up to 360 pA of  $I_A$  when depolarized to  $-24$  mV from a holding potential of  $-84$  mV. This current activated at membrane potentials between  $-54$  and  $-44$  mV in most cells, and occasionally at slightly more negative voltages (Fig. 3). The maximal slope conductance was reached by  $-24$  mV, and often at more negative potentials. Activation of  $I_A$  was rapid, with time-to-peak values of  $7 \pm 1$  ms in twenty-six cells that were stepped from  $-84$  to  $-24$  mV. Figure 2 shows no appreciable

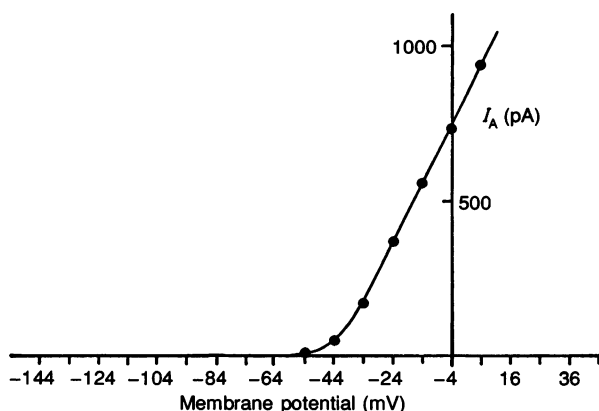


**Figure 3.** Peak current–voltage curve for  $I_A$ . The curve indicates the peak magnitude of  $I_A$  activated by a typical SHC when held at  $-84$  mV and depolarized to various membrane potentials. The isolation of  $I_A$  from other currents in the cell was accomplished by making use of the inactivating property of  $I_A$  as described in Methods. The curve was fitted by eye.

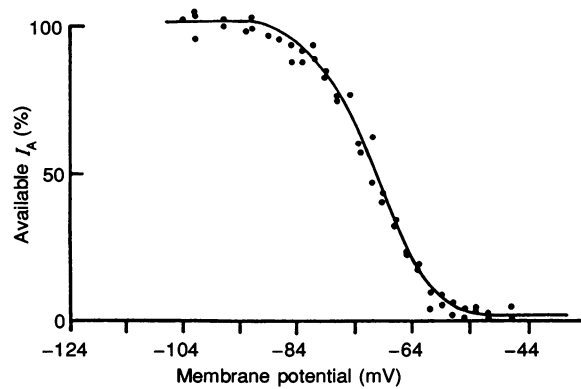


**Figure 4.** Inactivation curve for  $I_A$

The amount of  $I_A$  (% of total) available to a typical SHC is plotted relative to the membrane potential of the cell. The data points were determined using the following voltage protocol. The cell was stepped to various membrane potentials ( $V_m$ ) for 200 ms to alter the amount of inactivation of  $I_A$ , and then stepped to a test potential of  $-24$  mV to activate available  $I_A$  channels. The normalized peak value of  $I_A$  that was generated by this protocol was plotted as a function of  $V_m$ . The curve represents a Boltzmann distribution of the form  $I/I_{\max} = 1/(1 + \exp[(V_m - V_{1/2})/k])$ , where  $I/I_{\max}$  is the percentage of peak current available at the stated holding potential,  $V_m$ .  $V_{1/2}$  is the membrane potential at which half of the channels were in an inactivated state and  $k$  is the slope factor describing the voltage dependence of inactivation ( $V_{1/2} = -71$  mV and  $k = 4.9$  mV for the above curve). The curve was fitted to the data points minimizing the least squares difference.

change in the time to peak  $I_A$  at different voltages. The voltage dependence and rate of activation were similar among all of the cells that expressed  $I_A$ .

$I_A$  inactivation was both time and voltage dependent. In thirty cells that were voltage clamped at  $-84$  mV and stepped to  $-24$  mV,  $I_A$  was completely inactivated within  $73 \pm 16$  ms of the start of the voltage step.  $I_A$  channels were completely inactivated at membrane potentials positive to  $-56 \pm 5$  mV ( $n = 10$ ) and 50% inactivated at  $-74 \pm 5$  mV (Fig. 4). Complete removal of inactivation required membrane potentials more negative than  $-100$  mV. The removal of inactivation was also time dependent (Fig. 5), such that 50% of inactivation was removed after 44 ms at  $-84$  mV. Time periods greater than 150 ms were required to de-inactivate all the channels

available at this membrane potential. These properties of  $I_A$  inactivation were similar in all cells examined.

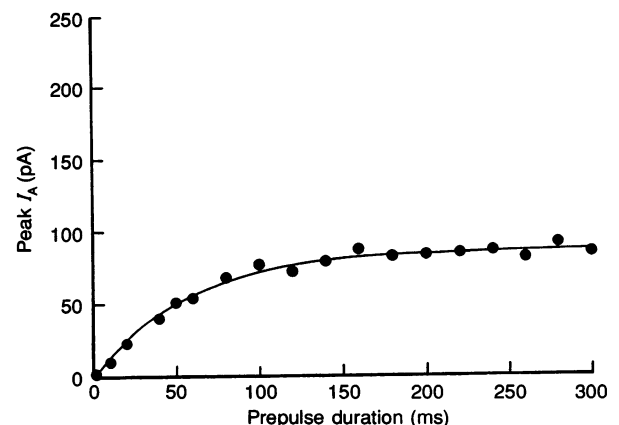
The sensitivity of  $I_A$  to 4-AP was examined with a dose-response experiment (Fig. 6). Half-block occurred at  $0.45$  mM 4-AP, while  $0.2$  mM 4-AP blocked 27% of the total  $I_A$  and  $10$  mM 4-AP blocked 98% of it.  $I_A$  in chick hair cells was insensitive to  $10$  mM TEA and did not diminish upon removing  $\text{Ca}^{2+}$  from the extracellular saline solution.

### Preferential expression of $I_A$ by shorter hair cells

While the intrinsic properties of  $I_A$  appeared to be the same in all hair cells, the magnitude of  $I_A$  varied greatly. To study the amplitude of  $I_A$  in cells from different positions in the basilar papilla, cells were held at  $-84$  mV

**Figure 5.** Time dependence of removal of  $I_A$  inactivation

The amount of  $I_A$  generated by a SHC is plotted as a function of the length of time that the cell was at a membrane potential that removed inactivation from  $I_A$  channels. Specifically, the cell was held at a membrane potential of  $-34$  mV that inactivated all  $I_A$  channels, then for various time periods hyperpolarized to  $-84$  mV to remove inactivation, and finally stepped to  $-24$  mV to activate the  $I_A$  channels that were de-inactivated. The peak  $I_A$  value generated is plotted relative to the time the cell was held at  $-84$  mV. The curve was generated using the equation  $I = I_{\max}(1 - \exp[-T/\tau])$ , where  $I$  is the peak  $I_A$  generated for the time  $T$  at  $-84$  mV.  $I_{\max}$  is the maximal amount of peak  $I_A$  capable of being generated, and  $\tau$  is an exponential time constant. ( $I_{\max} = 87$  pA and  $\tau = 58.7$  ms for the above curve).



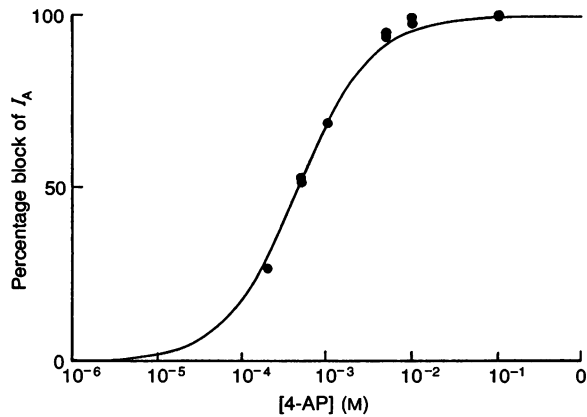


**Figure 6. Sensitivity of  $I_A$  to 4-AP**

The percentage of  $I_A$  blocked by various concentrations of 4-AP is displayed on a semilogarithmic plot. The data points were obtained from a total of 3 cells. The curve was derived using the Michaelis–Menten equation (half-block concentration = 0.45 mM), and the goodness of fit was determined by the least squares method ( $r^2 = 0.992$ ).

for at least 500 ms to remove inactivation and then depolarized to  $-24$  mV to activate  $I_A$ . The same voltage steps were then applied in the presence of 10 mM 4-AP. The amplitude of  $I_A$  in each cell was taken as the peak value of the 4-AP-sensitive current (Fig. 2 in Murrow & Fuchs, 1990). The parameters chosen to study  $I_A$  were based upon the following. First, at  $-84$  mV more than 90% of inactivation was removed from  $I_A$  channels (Fig. 4). More negative holding potentials that would have completely removed inactivation were not used because

these levels would have elicited large inward rectifier currents in taller hair cells, making them difficult to voltage clamp. Second, virtually all of the available  $I_A$  channels were activated at  $-24$  mV (Fig. 3). Third, since more than 500 ms separated depolarizing stimuli, the time dependence of inactivation removal (Fig. 5) ensured that the  $I_A$  channels that were inactivated by the previous test step had sufficient time to recover from this inactivation. Finally, virtually all of the  $I_A$  expressed by the cells was blocked by 10 mM 4-AP (Fig. 6). Higher concentrations of

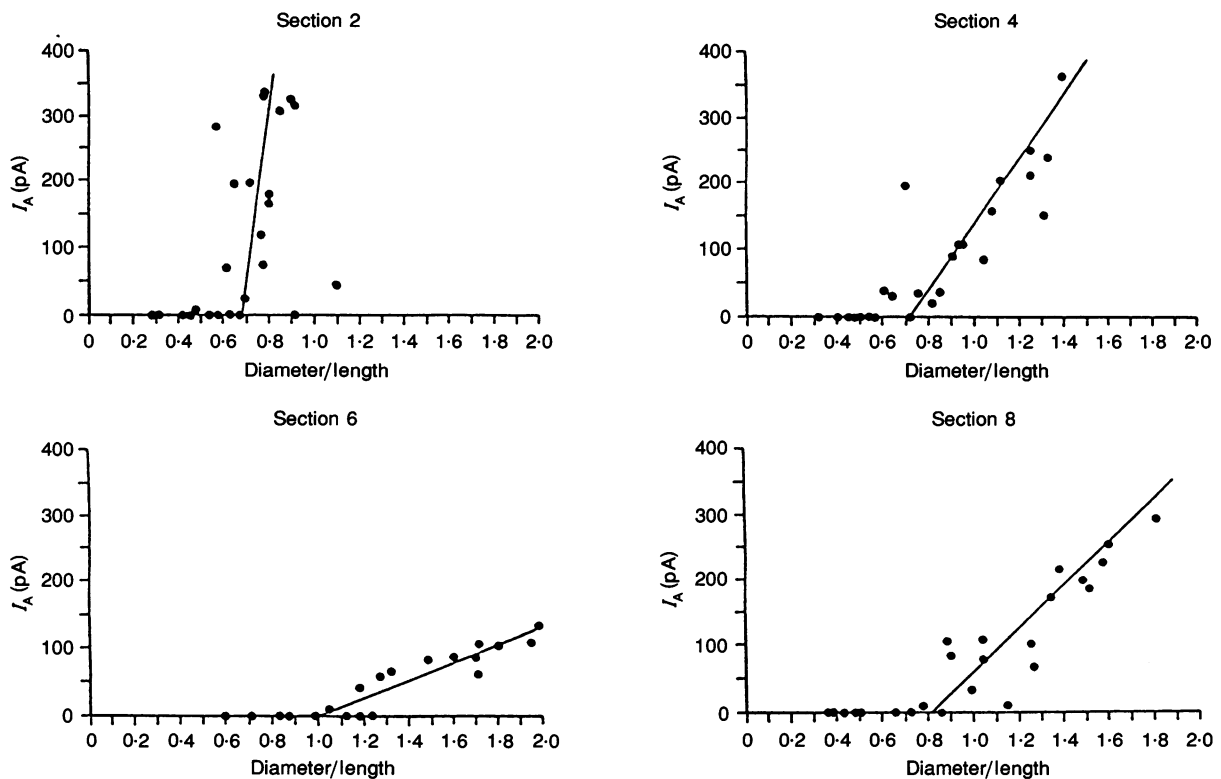


**Figure 7. Magnitude of  $I_A$  plotted as a function of cell morphology in section 2 (200–400  $\mu\text{m}$  from the apical tip), section 4 (600–800  $\mu\text{m}$ ), section 6 (1000–1200  $\mu\text{m}$ ) and section 8 (1400–1600  $\mu\text{m}$ )**

Cell morphology is represented by the ratio of apical diameter of a cell to its length. Linear regression lines were fitted to data points greater than 0.48 (section 2), 0.60 (section 4), 0.75 (section 6) and 1.00 (section 8).

Table 2. Range of isolated cell morphologies

	Section 2		Section 4		Section 6		Section 8	
	Diameter	Length	Diameter	Length	Diameter	Length	Diameter	Length
Maximum	12.3	30.0	13.2	28.2	16.2	22.8	17.7	12.0
Minimum	7.2	11.1	8.4	9.0	7.8	8.4	7.2	6.6

Measurements shown are in  $\mu\text{m}$ .

this drug affected channel types other than those responsible for  $I_A$ .

Even 10 mM 4-AP was not totally free of effects on other currents. The minor effects of 4-AP on non- $I_A$  currents occasionally revealed a small 4-AP-sensitive current that was not believed to be  $I_A$  because it did not inactivate at  $-54$  mV. Therefore, small 4-AP-sensitive currents ( $< 50$  pA) were deemed to be  $I_A$  only if they rapidly activated and inactivated at more positive potentials.

$I_A$  was studied in cells isolated at distances of 200–400  $\mu\text{m}$  (section 2), 600–800  $\mu\text{m}$  (section 4), 1000–1200  $\mu\text{m}$  (section 6), and 1400–1600  $\mu\text{m}$  (section 8) from the apical tip of the basilar papilla (Fig. 1). Cells from these locations exhibited a wide range of morphologies (Table 2). Differently shaped cells expressed different amounts of  $I_A$  (Fig. 7). The morphological parameter used to describe cell shape was the ratio of the apical diameter of the cell to its length. This parameter was chosen since both the length and apical diameter varied in the cells studied. Furthermore, this morphological ratio has previously been used to divide chick hair cells into two subtypes (Tanaka & Smith, 1978). According to this classification, THCs have a morphological ratio  $< 1$ , while SHCs have a ratio  $> 1$ . In Fig. 7, it is convenient to think of the cells as becoming 'shorter' when

moving to the right along the morphology axes; that is to say, the apical surface diameter of the cells increases while their length decreases. In all of the sections, the tallest hair cells had no  $I_A$ . Of the cells that did express  $I_A$ , the magnitude of this current varied as a continuous function of cell shape. Shorter hair cells expressed more of this current.

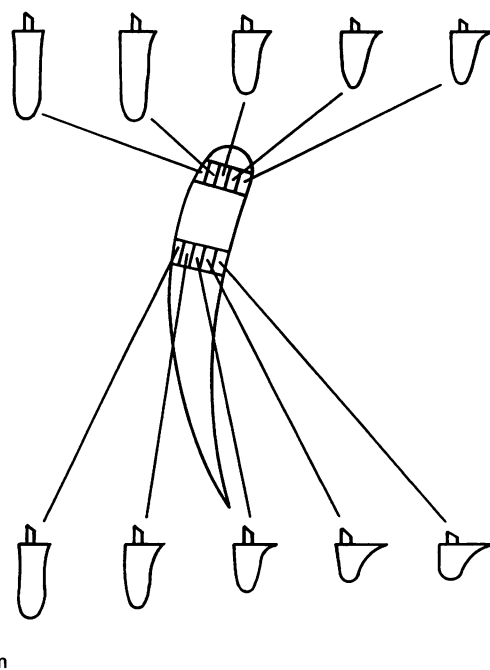
Despite these gross similarities, there were two primary differences found among the sections. First, the range of cell shapes that did not express  $I_A$  was larger in more basally located sections. Second, the 'steepness' of the  $I_A$  gradient varied between sections (Fig. 7). For cells with the same morphological ratio, those located nearer to the apical tip of the cochlea usually expressed more  $I_A$  than those more basally positioned.

However, this trend did not hold true for cells at the most apical tip of the basilar papilla. All cells isolated from 0–200  $\mu\text{m}$  from the tip of the basilar papilla (section 1) failed to express  $I_A$ . The eleven cells studied from this area exhibited a wide range of morphologies (morphological ratios spanning from 0.27 to 0.83).

SHCs were found to have a resting membrane potential more depolarized than THCs (SHC:  $-44 \pm 9$  mV,  $n = 24$ ; THC:  $-51 \pm 14$  mV,  $n = 48$ ;  $P < 0.05$ ). However, resting

Figure 8. Cell shape according to cross-cochlear position in section 2 and 6

The curved structure is the sheet of hair cells that makes up the basilar papilla (the shaded area in Fig. 1). Both sections 2 and 6 are divided into segments that are 20% of the total distance across the width of the basilar papilla. The cell drawn for each segment is meant to represent the morphology of the cells in that segment. The dimensions of these cell cartoons were based upon the representative apical surface diameter and length of the cells for each segment. The determination of these size parameters is described in the text and the scale bar refers only to them.



potentials of the cells with  $I_A$  did not correlate with the magnitude of  $I_A$  expressed by the cells ( $P > 0.05$ )

### Preferential expression of $I_A$ by cochlear position

The differences in  $I_A$  expression along the chick cochlea prompted a study of  $I_A$  expression according to cross-cochlear position, which could be determined by morphological criteria that vary across the width of the chick cochlea (Hirokawa, 1978; Tanaka & Smith, 1978). A light microscopic study on the intact cochlea was subsequently carried out to determine the cross-cochlear position of a cell based on its morphology.

The representative morphology of cells across the cochlea in sections 2 and 6 is shown in Figs 8 and 9A. The morphological parameter in Fig. 9, the ratio of the apical diameter to cell length, is the same as that used to describe cells in the electrophysiology experiments. In both sections 2 and 6, the tallest hair cells (smallest morphological ratio) were positioned on the neural side of the cochlea, that is the side closest to the exit site of the cochlear nerve. Moving across the cochlea, the diameter-to-length ratio of the cells increased. This morphological change across the cochlea involved both variation in cell length and apical surface diameter as suggested by previous reports (Hirokawa, 1978; Tanaka & Smith, 1978). In section 2, the representative

length of the cells in each population ranged from 15 to 27  $\mu\text{m}$ , while in section 6 they ranged from 12 to 23  $\mu\text{m}$ . Ranges for representative apical surface diameter of cells in sections 2 and 6 were 8–13  $\mu\text{m}$  and 9–20  $\mu\text{m}$ , respectively. In both sections, cell length decreased and cell apical surface diameter increased in the direction from neural to abneural.

The major difference between the two sections was in the rate of change in shape across the cochlea. In sections 2 and 6, the width of the basilar papilla was similar (411  $\mu\text{m}$  and 423  $\mu\text{m}$  respectively), as were the number of hair cells spanning each cochlear width (42 and 38 respectively). Over the same distance (or number of cells moved across the cochlea), the morphology of the cells (apical diameter/length) changed to a greater degree in section 6.

Combining the data relating  $I_A$  to cell shape (Fig. 7) with those relating cell shape to cross-cochlear position (Fig. 9) provided an estimate of the magnitude of  $I_A$  expressed by a cell according to cross-cochlear position (Fig. 9B). A population of taller hair cells that had no  $I_A$  were found on the neural side of the cochlea in both sections 2 and 6. Specifically in section 2, cells with a morphological ratio of less than 0.57 did not reveal significant amounts of  $I_A$  and these cells occupied about the first 40% of the distance across the cochlea from the neural side. Cells in section 6 with a ratio less than about

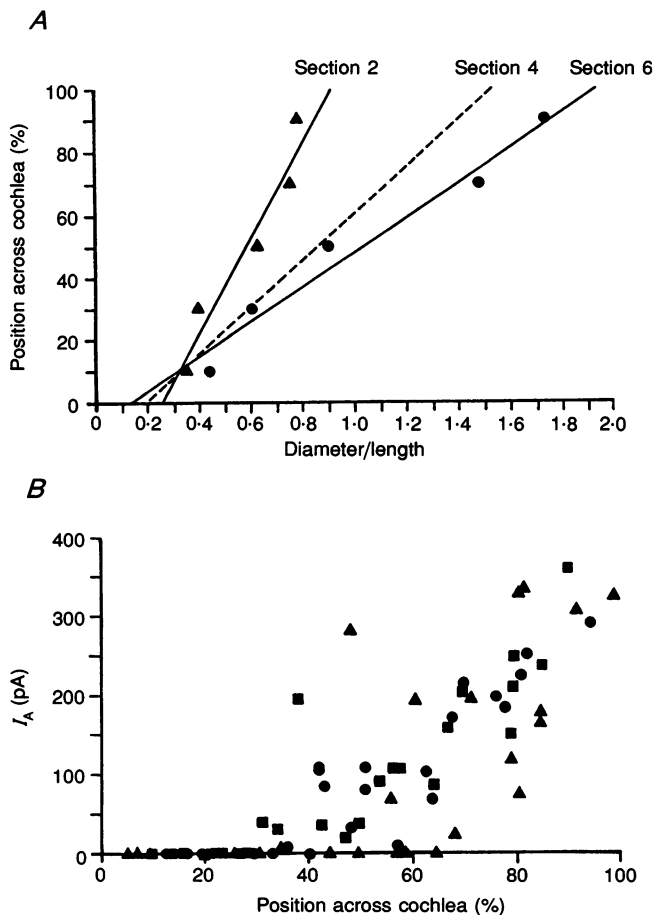


**Figure 9.** Relationships between cell shape (apical cell diameter/cell length), cross-cochlear position and  $I_A$  expression for sections 2, 4 and 6

*A*, cell position is plotted as a percentage of the total distance across the cochlea with 0% representing the superior side (neural edge). Each data point for sections 2 and 6 is a mean of values from two cochleas studied. The continuous lines drawn were fitted by linear regression ( $r^2 = 0.93$  for section 2;  $r^2 = 0.97$  for section 6). The dashed line represents an estimate of the relationship between cell shape and cross-cochlear position in section 4. It was derived by assuming that the tallest and shortest cells studied in section 4 came from near extreme cochlear positions and, as in sections 2 and 6, a linear relationship existed between the extremes. The cell shapes for the tallest and shortest cells were assigned 10 and 90% cross-cochlear positions, respectively, since there might not have been a full range of cell shapes isolated. *B*, using the relationships in *A*, the data in Fig. 7 were used to generate this plot of  $I_A$  expression relative to cross-cochlear position ( $\blacktriangle$  = section 2;  $\blacksquare$  = section 4;  $\bullet$  = section 6).



0.89 had no significant amounts of  $I_A$  and these cells were also found to be positioned within about 40% of the distance from the neural side of the cochlea. The remaining 60% of the distance across the cochlea, in both sections, provided cells that expressed  $I_A$ , and the cells that were positioned closer to the abneural side expressed more of this current.

An estimate of the relationship between  $I_A$  and cross-cochlear position in section 4 also supported the results from sections 2 and 6. The dashed line in Fig. 9A is an estimate of the relationship between cell shape and cross-cochlear position (see figure legend for derivation) and was used to generate the relationship between  $I_A$  and cochlear position for section 4.

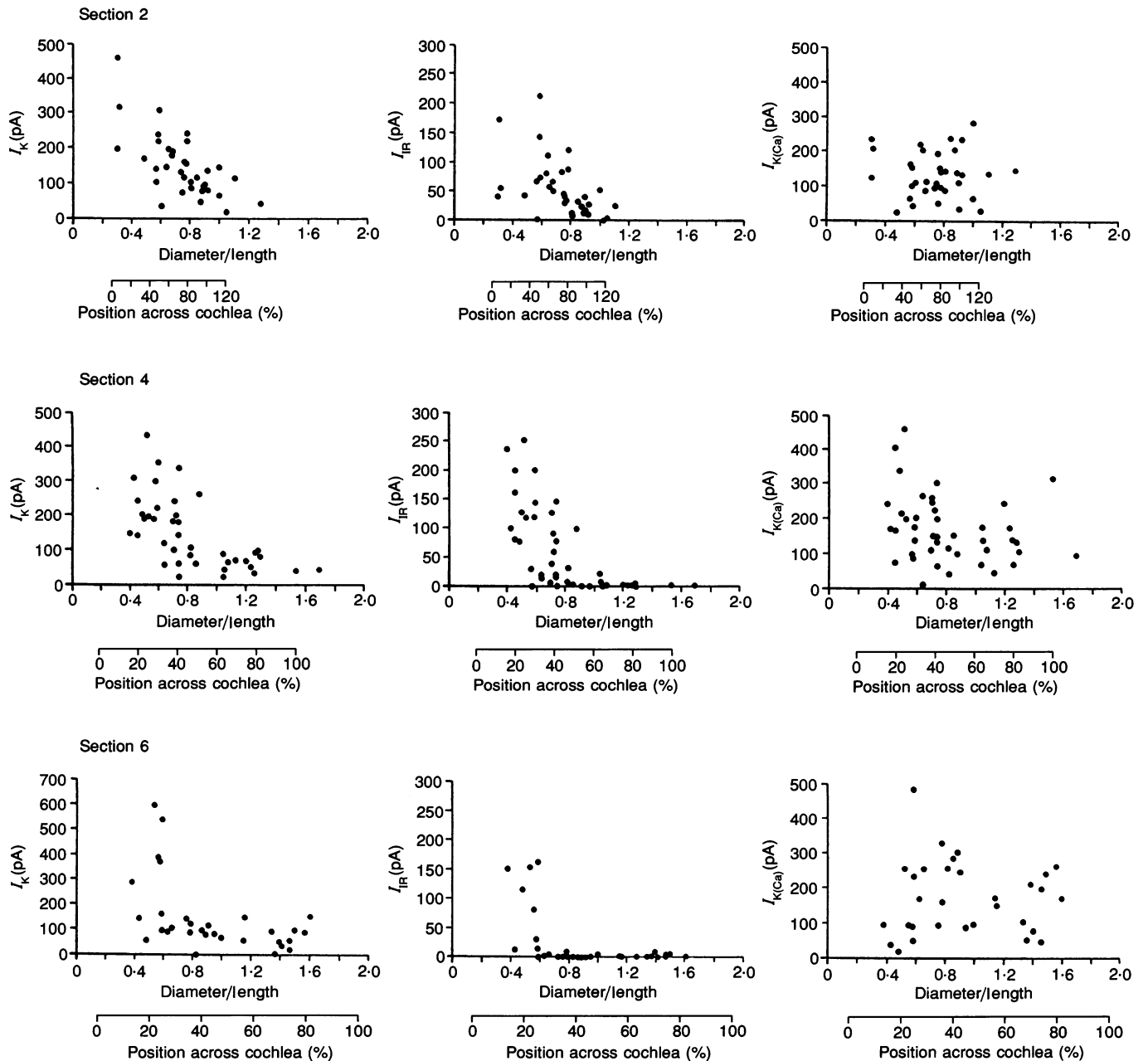


**Figure 10. Expression of  $I_K$  (left),  $I_{IR}$  (middle), and  $I_{K(Ca)}$  (right) as a function of cell shape and cross-cochlear position in sections 2 (top), 4 (middle) and 6 (bottom)**

The magnitude of  $I_K$ ,  $I_{IR}$  and  $I_{K(Ca)}$  were measured as described in the Methods. The morphological axis (apical cell diameter/cell length) is the same in all plots and the same as used for  $I_A$  plots in Fig. 7. Below each morphology axis, a cross-cochlear position axis is supplied. The superior side (neural edge) of the basilar papilla is represented by 0%. This position axis was generated using the relationships between cell shape and cross-cochlear position in Fig. 9A.

The results from all three sections are consistent with the hypothesis that cells located at similar positions across the width of the cochlea express similar amounts of  $I_A$ . For example, four cells that expressed a mean of 184 pA of  $I_A$  in section 2, 190 pA in section 4, and 193 pA in section 6 had mean morphological ratios of 0.75, 1.19 and 1.44 respectively. Based upon the relationships in Fig. 9A, these cells were located about 75% of the distance across the cochlea from the neural side in all three sections. In Fig. 9B, the similarity in the relationship between  $I_A$  and cross-cochlear position is clear between the three sections. The greater variance in section 2 might in part be expected since the  $I_A$ -morphology and morphology-position relationships used to generate the results for section 2 in Fig. 9B were the steepest of all the sections; any variance in cell shape in section 2 resulted in a larger change in the estimate of cross-cochlear position as compared to that in other sections.

### Preferential expression of other hair cell currents

Other types of potassium current found in chick hair cells included  $I_K$ ,  $I_{IR}$  and  $I_{K(Ca)}$ . Estimation of the amount of  $I_K$  and  $I_{K(Ca)}$  and direct measurement of  $I_{IR}$  magnitude in cells were made as outlined in the Methods.  $I_K$  and  $I_{IR}$  were preferentially expressed among hair cells of different shape and different position across the width of the basilar papilla. Under the recording conditions employed, the taller hair cells, which were positioned nearer to the neural edge, in each of sections 2, 4 and 6 had the most  $I_K$  and  $I_{IR}$  (Fig. 10). The expression of these currents by the taller hair cells was in contrast to the preferential expression of  $I_A$  by the shorter hair cells (Figs 7 and 10). In sections 4 and 6 particularly, expression of significant amounts of both  $I_K$  and  $I_{IR}$  was mutually exclusive with expression of  $I_A$ . In contrast to  $I_K$  and  $I_{IR}$ ,  $I_{K(Ca)}$  expression did not vary significantly among populations of hair cells (Fig. 10). Accordingly, cells with  $I_A$  often had  $I_{K(Ca)}$ .

## DISCUSSION

This study examined ion channels in chick cochlear hair cells and found a systematic variation according to position across the width of the cochlea. A rapidly inactivating outward current was identified as an A-type current. At various levels along the length of the cochlea, the expression of this current correlated with cell morphology and with cross-cochlear position. The tallest hair cells, located on the neural side of the cochlea, showed none of this current, while the shortest cells, on the other side, exhibited large amounts. A gradient of expression was evident among cells with  $I_A$ , such that shorter hair cells positioned nearer to the abneural side of the cochlea had more of this current. Except for the very distal tip of the basilar papilla, this gradient was similar at various locations along the length of the cochlea.  $I_A$  iso-magnitude lines appear to run

parallel to the long axis in the apical half of the cochlea. The differences then seen between  $I_A$  and cell shape at levels along the length of the cochlea appear to be a reflection of the different distribution of cell shapes across the cochlea at those levels. In addition to  $I_A$ , other currents such as  $I_K$  and  $I_{IR}$  were also found to be differentially distributed among hair cells across the cochlea.

### Characteristics of $I_A$

A rapidly inactivating potassium current was first seen in molluscan neurons by Hagiwara, Kusano & Saito (1961). Connor & Stevens (1971) studied this current in detail and termed it 'A-current'. Subsequently,  $I_A$  has been found in a wide variety of animals and types of cells (reviewed in Rudy, 1988). The kinetic and voltage-dependent properties of  $I_A$  in chick hair cells are similar to those of  $I_A$  found in ganglion cells of *Anisodoris* and *Tritonia* (Connor & Stevens, 1971; Thompson, 1977), bag cell neurons of *Aplysia* (Kaczmarek & Strumwasser, 1984; Strong, 1984), sympathetic neurons of the bullfrog (Adams, Brown & Constanti, 1982), and larval brain and ganglion neurons of *Drosophila* (Solc, Zagotta & Aldrich, 1987).

In addition to the present report,  $I_A$  has also been identified in other hair cells, including those of the bullfrog sacculus (Lewis & Hudspeth, 1983; Hudspeth & Lewis, 1988), the semicircular canal of frogs (Housley, Norris & Guth, 1989), the semicircular canal and utricle of the pigeon (Lang & Correia, 1989), and the fish saccule (Sugihara & Furukawa, 1989). All of these hair cells are of vestibular origin, while the present report describes  $I_A$  in auditory hair cells. The  $I_A$  in chick hair cells is similar to that found in other vertebrate hair cells, and most similar to that in bullfrog saccular cells. Notably, in both chick auditory and bullfrog saccular hair cells,  $I_A$  differs from that in cells of other animals by its unavailability at the resting potential of the cell.  $I_A$  in chick and bullfrog hair cells is inactivated at rest, whereas this is not the case in frog semicircular canal, pigeon semicircular canal and goldfish saccular cells. In chick hair cells, little if any  $I_A$  is available for activation from the average resting potential of  $-46$  mV.

### Preferential expression of $I_A$

Expression of  $I_A$  in the bird cochlea is tightly coupled to cell shape and, more precisely, to cross-cochlear position. Two other reports have addressed differential expression of this type of current among cells of a single organ. First, 'oscillatory-type' cells from caudal positions in the goldfish saccule have  $I_A$ , while those from rostral areas tend not to exhibit this current (Sugihara & Furukawa, 1989). Second, consistent differences in peak magnitude, density and inactivation kinetics of  $I_A$  have been observed between identifiable ganglion cells in molluscs (Serrano & Getting, 1989). The functional significance of these findings have not yet been explored.

What could be responsible for the differences in magnitude of  $I_A$  that are seen among cells across the width

of the bird cochlea? The variation does not appear to be due to intrinsic differences in the voltage dependence of  $I_A$  channels in cells. Under the recording conditions used to examine  $I_A$ , the amounts of  $I_A$  measured were a good representation of the maximal amount of this current that the cell was capable of generating. Holding the cells at  $-84$  mV for 500 ms prior to activating the  $I_A$  channels was sufficient to remove inactivation from virtually all of the channels. Similarly, all of the  $I_A$  channels that had inactivation removed at  $-24$  mV were in a conducting state and any minor variations in the voltage dependence of activation would not affect the measurement of  $I_A$ . Therefore, the variation in  $I_A$  magnitude among cells is likely to be due to either differences in numbers of  $I_A$  channels or differences in single channel conductance. The latter is less likely because the similarity of voltage-dependent and kinetic properties from one cell to the next suggests a homogeneous population of channels. Also, since the shorter hair cells express more  $I_A$ , it is unlikely that all of the cells contain the same density of channels in their cell membrane and the different amounts of current are due to different amounts of cell membrane. All of the ion channels in hair cells, except for the mechanical transduction channels in the stereocilia, are located in the basolateral membrane (Roberts, Jacobs & Hudspeth, 1990). Clearly the shorter hair cells have less basolateral membrane than taller hair cells, yet they express more  $I_A$ . Therefore, assuming that single channel conductances are the same for all of the channels, the differences seen in the magnitude of  $I_A$  are most probably due to differences in absolute numbers of  $I_A$  channels in the cell. Thus, shorter hair cells are likely to have a higher density of these channels in their membrane.

The absence of  $I_A$  in cells from the most apical tip of the basilar papilla is intriguing. The morphology of cells isolated from this area overlapped those of cells in section 2. The trend of  $I_A$  expression in sections 2, 4, 6 and 8 predict that at least some of the cells studied in section 1 should have  $I_A$ . There is no reason to believe that any less of a representation of hair cells was isolated from this region as compared to other sections of the cochlea. The very distal (apical) tip of the chick basilar papilla has previously been described as anatomically unique from the rest of the papilla (Lavigne-Rebillard, Cousillas & Pujol, 1985). The 'atypical' sensory cells from this region were more similar to vestibular than to auditory receptor cells. The difference in  $I_A$  expression that was found in this region of the cochlea may preview physiological differences that future research will uncover between this area and the remainder of the auditory papilla.

### Relationship of $I_A$ to other hair cell currents

Other potassium currents described in chick hair cells include  $I_K$ ,  $I_{IR}$  and  $I_{K(Ca)}$  (Fuchs & Evans, 1990), as well as a cholinergic-gated current ( $I_{ACh}$ ; Murrow & Fuchs, 1990; Fuchs & Murrow, 1992*a, b*). Since  $I_A$  is generated by a

voltage-dependent channel, its contribution to hair cell physiology will be tightly intertwined with the other currents in that cell that shape the receptor potential. What other currents are expressed by cells that have  $I_A$ ? Estimates of the amount of  $I_K$  and direct measurement of  $I_{IR}$  revealed that these currents are differentially expressed by cells across the chick cochlea. However, their gradient of expression is opposite to that of  $I_A$ . Except for areas in the apex of the cochlea, cells with  $I_A$  have very little, if any,  $I_K$  and  $I_{IR}$ .  $I_{IR}$  has been postulated to contribute to the large negative resting potentials of THCs (Fuchs & Evans, 1990). The absence of  $I_{IR}$  in shorter hair cells that have more depolarized resting potentials is consistent with this idea.

$I_{K(Ca)}$  was often found in cells with  $I_A$ . In chick THCs,  $I_{K(Ca)}$ , in conjunction with  $I_{Ca}$ , is responsible for generating the electrical resonance (ringing) of these cells (Fuchs *et al.* 1988; Fuchs & Evans, 1990). Some chick SHCs have also been found to be electrically tuned (Murrow & Fuchs, 1989). Whether  $I_A$  is capable of influencing electrical tuning in these cells is not known. At least around the resting potential of the cell,  $I_A$  is not expected to influence the cell's receptor potential, since this current is completely inactivated in that voltage range. Before  $I_A$  can contribute to membrane electrical properties, the cell must first be hyperpolarized to remove inactivation from  $I_A$  channels.

A cholinergic-gated current that is co-expressed in hair cells with  $I_A$  could remove the inactivation from  $I_A$  channels (Murrow & Fuchs, 1990; Fuchs & Murrow, 1992*b*). This current probably underlies efferent inhibition of those cells. When acetylcholine (the proposed neurotransmitter at the efferent synapse onto hair cells) or carbachol (an acetylcholine agonist) is applied to isolated chick hair cells, the cells respond with a robust potassium current that is dependent upon an external source of  $Ca^{2+}$  (Murrow & Fuchs, 1990; Fuchs & Murrow, 1992*b*). This current is capable of hyperpolarizing the cell to near  $E_K$  (the reversal potential for potassium;  $-80$  mV), which could remove inactivation from  $I_A$  channels and make them available to the cell upon subsequent depolarization. Hence, the significance of  $I_A$  may lie in association with *post*-efferent inhibition of the cochlea.

Interestingly, the distribution of  $I_A$  and efferent processes appear similar. Preliminary experiments (Murrow & Fuchs, 1990) have found that the tallest hair cells, which have no  $I_A$ , had no physiological response to carbachol, while the majority of shorter hair cells with  $I_A$  were sensitive to carbachol. Furthermore, the hair cells at the apical tip of the basilar papilla that do not express  $I_A$  have few efferent contacts (Lavigne-Rebillard *et al.* 1985). Finally, a gradient has been described for efferent innervation across the bird cochlea, the shorter hair cells being somewhat more densely innervated by efferent processes (Firbas & Muller, 1983). These relations between  $I_A$  and efferent processes/responses are consistent with a functional link between the two.

## Significance of $I_A$ for cell function

What might be the role for  $I_A$  in hair cell function? Hair cells of the goldfish saccule have  $I_A$  with voltage-dependent inactivation that allows some  $I_A$  channels to be de-inactivated at the resting potential of the cell. Since hair cells from the goldfish produce 'ringing' voltage responses around their resting potential (Sugihara & Furukawa, 1989),  $I_A$  will contribute to membrane conductances in the voltage range that supports that electrical resonance. Blocking this current in goldfish cells with 4-AP eliminates the voltage oscillations (Sugihara & Furukawa, 1989). Since it is thought that  $I_A$  provides the main component of 'rectification' for these cells, eliminating it causes a large increase in the membrane time constant, and the electrical properties of the membrane no longer can support the resonant behaviour.

Similarly,  $I_A$  might provide a significant conductance to chick hair cells, but only after de-inactivation of the  $I_A$  channels. Efferent-induced hyperpolarization will shut down voltage-dependent currents such as  $I_{K(Ca)}$  and  $I_{Ca}$ , making the membrane highly resistive. Following efferent inhibition of the cell,  $I_A$  will turn on as the cell is depolarized and provide a voltage-dependent conductance to the cell in the voltage range  $-55$  to  $-45$  mV, a range in which the other types of voltage-dependent ion channels are not activated (Fuchs *et al.* 1988). Hence, the general effect of  $I_A$  could be to reduce the membrane time constant and allow the cell to follow sound input more accurately immediately following efferent stimulation.

## Hair cell functional specialization

The present results provide new information about hair cells in the chick cochlea and help clarify previous studies carried out on this organ. Earlier studies on chick THCs (Fuchs *et al.* 1988; Fuchs & Evans, 1990) emphasized differences in membrane properties of cells along the length of the cochlea. In general, the apical hair cells had  $I_K$  that could dominate the current-voltage relation, while more basal cells expressed primarily  $I_{K(Ca)}$ , with little or no  $I_K$  or  $I_{IR}$ . The present results indicate that the tallest hair cells from the middle of the cochlea can have a similar complement of ion channels to cells from the apex.

Differences in hair cell morphology and innervation have suggested that functional differences exist across the width of the avian cochlea. The distribution of  $I_A$ , as well as that of other currents, further confirms that different hair cells are functionally specialized. However, categorizing the hair cells in the bird cochlea has proven difficult. There are no distinct anatomical boundaries to delineate different hair cell types as in the mammalian cochlea. The present results of current distributions across the cochlea indicate that the classic classification as SHCs and THCs is not suitable for a functional division, as has been suggested also by innervation studies (von Düring, Andres & Simon, 1985).

Based upon the distribution of ion channels across the cochlea, how might the hair cells be categorized? With regard to the distribution of  $I_A$  in areas other than the extreme apical tip of the cochlea, differences appear to exist primarily according to cross-cochlear position. Distributions of  $I_K$  and  $I_{IR}$  also revealed great differences across the cochlea, but unlike  $I_A$ , these distributions with respect to cross-cochlear position changed at different levels along the length of the cochlea. For example, virtually all of the cells across the cochlea expressed  $I_K$  and  $I_{IR}$  in section 2, but in section 6 only a small population of the tallest hair cells had these currents. The significance of this variation is not understood. Nevertheless, a population of the tallest hair cells in each section along the length of the cochlea possessed a very similar complement of ion channels. These cells had no  $I_A$ , but instead had large amounts of  $I_{IR}$  and  $I_K$ , along with some  $I_{K(Ca)}$ ; they also had  $I_{Ca}$  (Fuchs, Evans & Murrow, 1990). Cells with these characteristics have large resting potentials and respond to stimuli from their resting potential with  $Ca^{2+}$  action potentials (Fuchs *et al.* 1988). Perhaps these cells can be thought of as receptor cells that correspond to mammalian inner hair cells. They are analogous to inner hair cells based upon ion channel composition (Kros & Crawford, 1990), position in the cochlea, and robust afferent innervation. It is intriguing then to speculate that the rest of the cells across the cochlea of the chick might serve some modulatory role like mammalian outer hair cells.

## REFERENCES

- ADAMS, P. R., BROWN, D. A. & CONSTANTI, A. (1982). M-currents and other potassium currents in bullfrog sympathetic neurons. *Journal of Physiology* **330**, 537–572.
- CONNOR, J. A. & STEVENS, C. F. (1971). Voltage clamp studies of a transient outward membrane current in gastropod neural somata. *Journal of Physiology* **213**, 21–30.
- FIRBAS, W. & MULLER, G. (1983). The efferent innervation of the avian cochlea. *Hearing Research* **10**, 109–116.
- FUCHS, P. A. & EVANS, M. G. (1990). Potassium currents in hair cells isolated from the cochlea of the chick. *Journal of Physiology* **429**, 529–551.
- FUCHS, P. A., EVANS, M. G. & MURROW, B. W. (1990). Calcium current in hair cells isolated from the cochlea of the chick. *Journal of Physiology* **429**, 553–568.
- FUCHS, P. A. & MURROW, B. W. (1992a). A novel cholinergic receptor mediates inhibition of chick cochlear hair cells. *Proceedings of the Royal Society B* **248**, 35–40.
- FUCHS, P. A. & MURROW, B. W. (1992b). Cholinergic inhibition of short (outer) hair cells of the chick's cochlea. *Journal of Neuroscience* **12**, 800–809.
- FUCHS, P. A., NAGAI, T. & EVANS, M. G. (1988). Electrical tuning in hair cells isolated from the chick cochlea. *Journal of Neuroscience* **8**, 2460–2467.
- HAGIWARA, S., KUSANO, K. & SAITO, N. (1961). Membrane changes in *Onchidium* nerve cell in potassium-rich media. *Journal of Physiology* **155**, 470–489.
- HIROKAWA, N. (1978). The ultrastructure of the basilar papilla of the chick. *Journal of Comparative Neurology* **181**, 361–374.
- HOUSLEY, G. D. & ASHMORE, J. F. (1992). Ionic currents of outer hair cells isolated from the guinea pig cochlea. *Journal of Physiology* **448**, 73–98.

- HOUSLEY, G. D., NORRIS, C. H. & GUTH, P. S. (1989). Electrophysiological properties and morphology of hair cells isolated from the semicircular canal of the frog. *Hearing Research* **38**, 259–276.
- HUDSPETH, A. J. & LEWIS, R. S. (1988). Kinetic analysis of voltage- and ion-dependent conductances in saccular hair cells of the bull-frog, *Rana catesbeiana*. *Journal of Physiology* **400**, 237–274.
- KACZMAREK, L. K. & STRUMWASSER, F. (1984). A voltage-clamp analysis of currents underlying cyclic AMP-induced membrane modulation in isolated peptidergic neurons of *Aplysia*. *Journal of Neurophysiology* **52**, 340–349.
- KROS, C. J. & CRAWFORD, A. C. (1990). Potassium currents in inner hair cells isolated from the guinea-pig cochlea. *Journal of Physiology* **421**, 263–291.
- LANG, D. G. & CORREIA, M. J. (1989). Studies of solitary semicircular canal hair cells in the adult pigeon. II. Voltage-dependent ionic conductances. *Journal of Neurophysiology* **62**, 935–945.
- LAVIGNE-REBILLARD, M., COUSILLAS, H. & PUJOL, R. (1985). The very distal part of the basilar papilla in the chicken: A morphological approach. *Journal of Comparative Neurology* **238**, 340–347.
- LEWIS, R. S. & HUDSPETH, A. J. (1983). Voltage- and ion-dependent conductances in solitary vertebrate hair cells. *Nature* **304**, 538–541.
- MARTY, A. & NEHER, E. (1983). Tight-seal whole-cell recording. In *Single-Channel Recording*, ed. SAKMANN, B. & NEHER, E., pp. 107–121. Plenum, New York.
- MURROW, B. W. & FUCHS, P. A. (1989). Electrical membrane properties of short hair cells from the chick's cochlea. *Association for Research in Otolaryngology* **12**, 136–137.
- MURROW, B. W. & FUCHS, P. A. (1990). Preferential expression of transient potassium current ( $I_A$ ) by 'short' hair cells of the chick's cochlea. *Proceedings of the Royal Society B* **242**, 189–195.
- ROBERTS, W. M., JACOBS, R. A. & HUDSPETH, A. J. (1990). Colocalization of ion channels involved in frequency selectivity and synaptic transmission at presynaptic active zones of hair cells. *Journal of Neuroscience* **10**, 3664–3684.
- RUDY, B. (1988). Diversity and ubiquity of K channels. *Neuroscience* **25**, 729–749.
- SERRANO, E. E. & GETTING, P. A. (1989). Diversity of the transient outward potassium current in somata of identified molluscan neurons. *Journal of Neuroscience* **9**, 4021–4032.
- SOLC, C. K., ZAGOTTA, W. N. & ALDRICH, R. W. (1987). Single-channel and genetic analyses reveal two distinct A-type potassium channels in *Drosophila*. *Science* **236**, 1094–1098.
- STRONG, J. A. (1984). Modulation of potassium current kinetics in bag cell neurons of *Aplysia* by an activator of adenylate cyclase. *Journal of Neuroscience* **4**, 2772–2783.
- SUGIHARA, I. & FURUKAWA, T. (1989). Morphological and functional aspects of two different types of hair cells in the goldfish sacculus. *Journal of Neurophysiology* **62**, 1330–1343.
- TANAKA, K. & SMITH, C. A. (1978). Structure of the chicken's inner ear: SEM and TEM study. *American Journal of Anatomy* **153**, 251–272.
- THOMPSON, S. H. (1977). Three pharmacologically distinct potassium channels in molluscan neurones. *Journal of Physiology* **265**, 465–488.
- VON DURING, M., ANDRES, K. H. & SIMON, K. (1985). The comparative anatomy of the basilar papillae in birds. In *Functional Morphology in Vertebrates*, ed. DUNCKER, H. R. & FLEISCHER, G., pp. 682–685. Gustav Fischer Verlag, Stuttgart, New York.
- YELLEN, G. (1982). Single  $\text{Ca}^{2+}$ -activated nonselective cation channels in neuroblastoma. *Nature* **296**, 357–359.

### Acknowledgements

I am indebted to Dr P. A. Fuchs for his advice and support. I thank Drs A. R. Martin, S. R. Levinson, and W. O. Wickelgren for their comments on earlier versions of this manuscript. I also thank Mr G. Tarver, Ms L. Stahl, Ms J. Lieber, Ms L. Brozo, and Ms S. Miki for their technical assistance. This work was supported by grant NS07083 from NINDS, grant DC00276 from NIDCD to P. A. Fuchs, and a Scholars Award from the University of Colorado.

Received 7 September 1992; accepted 4 May 1994.